Journal of AppliedMath 2024, 2(6), 1870.
https://doi.org/10.59400/jam1870

Article

Analysis and modelling of the transmission dynamics of tuberculosis in the presence of latent and active populations

Aliyu Ibrahim[1,*], Mahdi Audu Janda[1], Stella Nyambura Kahianyu[1], Ass Gueye[1], Peter Chola Nkandu[1], Eugene Tettey Ayerkain[2]

[1] Department of Mathematics, African Institute for Mathematical Sciences (AIMS), Mbour 23000, Senegal
[2] Department of Mathematics, African Institute for Mathematical Sciences (AIMS), Accra GA027, Ghana
*** Corresponding author:** Aliyu Ibrahim, aliyu.ibrahim@aims-senegal.org

CITATION

Ibrahim A, Janda MA, Kahianyu SN, et al. Analysis and modelling of the transmission dynamics of tuberculosis in the presence of latent and active populations. Journal of AppliedMath. 2024; 2(6): 1870. https://doi.org/10.59400/jam1870

ARTICLE INFO

Received: 14 October 2024
Accepted: 24 December 2024
Available online: 18 November 2024

Abstract: Tuberculosis, a chronic infectious disease caused by *Mycobacterium tuberculosis*, remains a significant global health challenge, particularly in developing countries. This project investigates the dynamic transmission of tuberculosis, focusing on the interplay between latent and active populations. We develop and analyze an (Susceptible, Latent, Infectious, Recovered) compartmental mathematical model to examine key parameters affecting TB transmission dynamics. Our study employs stability and sensitivity analyses to provide critical insights into the basic reproduction number and equilibrium points of the TB transmission model. Through numerical simulations, we explore how various intervention strategies impact the spread of tuberculosis. The model yields an approximate reproduction number of 0.3, suggesting that under the current conditions represented in the model, TB would naturally decline in the population. Key findings emphasize the importance of maintaining a low transmission rate and improving the recovery rate to expedite the elimination of tuberculosis. The model demonstrates the complex interplay between susceptible, infected, latent, and recovered populations over time, highlighting the persistent nature of TB due to factors such as latent activation and loss of immunity in recovered individuals. This project provides a robust foundation for public health strategies aimed at controlling and ultimately eliminating tuberculosis. Our results underscore the need for targeted interventions focusing on reducing transmission, managing latent infections, and enhancing treatment efficacy. These insights can inform policy decisions and resource allocation in TB control programs, contributing to the global effort to combat this persistent disease.

Keywords: tuberculosis; latent population; reproduction number; sensitivity; stability

1. Introduction

The study of infectious disease dynamics is an essential field of mathematics for understanding how these diseases emerge in populations. Infectious diseases continue to severely affect human and animal populations in Africa and around the world, likely due to a lack of understanding of their dynamics. Despite increased efforts by governments and organizations to Project and control the spread of infectious diseases, they continue to spread and establish themselves in various region globally [1].

Moreover, tuberculosis has such a high death rate in humans, it remains a major global health issue and is one of the leading causes of death in most sub-Saharan African countries [2]. Tuberculosis (TB) is an ancient infectious disease caused by the bacteria

called Mycobacterium tuberculosis [3].

It primarily affects the lungs but can also impact other organs. Throughout history, TB has been a significant cause of mortality, potentially claiming more lives than any other microbial pathogen [4]. In 2022, TB was responsible for 1.3 million deaths globally, including 167,000 among individuals with HIV. An estimated 10.6 million people contracted TB, spanning different demographics [1].

TB remains a global public health challenge, ranking as the second leading cause of death worldwide after COVID-19. Despite its widespread presence across all countries and age groups, TB is treatable and preventable. Approximately a quarter of the world's population carries latent TB infection, with only a small percentage developing active TB disease.

If left untreated, TB can persist for a lifetime, leading to the formation of tubercles in various body parts [1]. The disease is believed to be transmitted through coughing, singing, kissing and sneezing from an infected individual with TB disease where by the pulmonary tuberculosis is spread as a droplet, with the frequency and duration of contact also make the risk of transmission of the disease increased [5].

Tuberculosis is commonly transmitted from an infected person to a susceptible or possibly latently infected individual through droplets produced when someone with active TB coughs, sneezes, or talks. These droplets contain the tuberculosis bacteria and can infect others nearby [6].

Tuberculosis infection can also spread through using eating and drinking utensils (such as dishes, cups, spoons, glasses) that belonged to an infected person if they were not properly sterilized. While TB mainly affects the lungs in pulmonary TB, it can also attack other parts of the human body. This includes the central nervous system, the circulatory system, the reproductive system, the bones and joints, and also the skin [7].

Tuberculosis remains one of the deadliest infectious diseases worldwide, continuing to claim numerous lives, particularly in Africa and other developing regions. The World Health Organization (WHO) reported in 2021 that tuberculosis caused approximately 1.6 million deaths globally, with a significant portion occurring in Africa [1]. Mathematical models generally explain the transmission dynamics of diseases and can predict the future status of these diseases. Models help identify the factors responsible for occurrence of diseases and the possible ways of combating these diseases in a dynamical system [8–12].

2. Model formulation and description

In the model, we divide the total population at any given time (t) into four sub-population known as compartment, with respect to their individual epidemic level and parameters as described in **Tables 1** and **2**.

Table 1. Variables and their description.

Variables	Description
$S(t)$	The susceptible population are those at the risk of contacting the infection from the bacteria (*mycobacteria*).
$L(t)$	Latent individuals; the compartment of the free-infectious stage. In this stage, individuals are infected but show no symptoms of the bacteria. The bacteria are not active, and they cannot transmit the disease to others.
$I(t)$	The actively infected population; this compartment includes all individuals showing symptoms of tuberculosis and who can transmit the disease to others.
$R(t)$	Recovered; these are individuals who have already recovered from tuberculosis and have temporary immunity.

Hence, the total population is now given as:

$$N(t) = S(t) + L(t) + I(t) + R(t) \tag{1}$$

The parameters used in the model in **Figure 1** are described in **Table 2**:

Table 2. Parameters and their descriptions.

Parameter	Description
π	Recruitment/incidence rate
β	Contact infections rate
μ	Natural death rate
λ	Rate of transmission (susceptible to latent)
τ	Progression rate (latent to infected)
δ	Death due to active tuberculosis
σ	Recovery rate (latent to recovered)
γ	Recovery rate (actively infected to recovered)
ϕ	Re-infection rate (recovered to susceptible)

The following ordinary differential equations were obtained from the model.

$$\begin{cases} \frac{dS}{dt} = \pi - \beta SI - \mu S - \lambda SL + \phi R \\ \frac{dI}{dt} = \beta SI - \gamma I - \mu I - \delta I + \tau L \\ \frac{dL}{dt} = \lambda SL - \mu L - \tau L - \sigma L \\ \frac{dR}{dt} = \gamma I - \mu R - \phi R + \sigma L \end{cases} \tag{2}$$

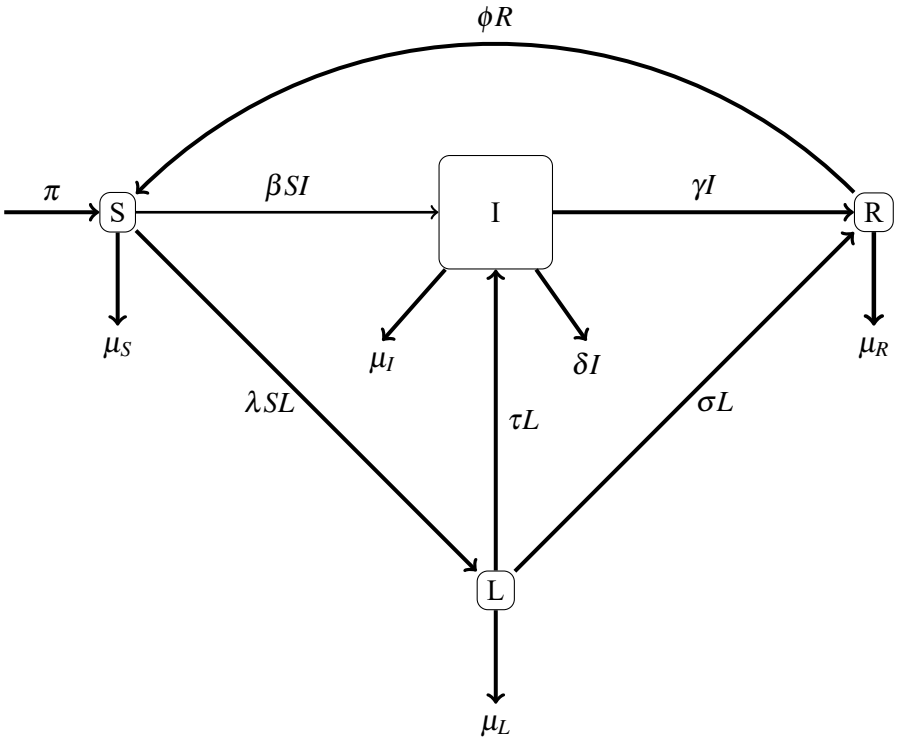

Figure 1. SLIR model flow diagram, with latent and infected (active) compartment.

3. Model analyses

3.1. Positivity and boundedness of solution

This section focuses on demonstrating that the solutions or trajectories of the system remain non-negative, which is essential since the model represents human populations. It is crucial to ensure non-negativity because negative values are not meaningful in the context of epidemiological modeling [13].

To establish positivity, we must show that if $S(0) \geq 0$, $I(0) \geq 0$, $L(0) \geq 0$, and $R(0) \geq 0$ initially, then $S(t) \geq 0$, $I(t) \geq 0$, $L(t) \geq 0$, and $R(t) \geq 0$ for all $t \geq 0$.

$$\frac{dS}{dt} = \pi - \beta SI - \mu S - \lambda SL + \phi R$$

Rewriting the equation in a standard form:

$$\frac{dS}{dt} = \pi - (\beta I + \mu + \lambda L)S + \phi R$$

When $S(t) \to 0$ and $R(t) \to 0$:

$$\frac{dS}{dt} \geq 0$$

We can conclude that, $S(t) \geq 0 \; \forall \, t$. Using the same approach, we can conclude that, the other variables are also positive.

To demonstrate that the dynamical system is uniformly bounded within the appropriate subset $\theta \subset \mathbb{R}^{+4}$, consider the total human population at any given time t, which is expressed as:

$$N(t) = S(t) + L(t) + I(t) + R(t)$$

The rate of change of the total population is given by:

$$\frac{dN}{dt} = \frac{dS}{dt} + \frac{dL}{dt} + \frac{dI}{dt} + \frac{dR}{dt}$$

Substituting the differential equations for each compartment, we get:

$$\begin{aligned}\frac{dN}{dt} &= \pi - (\beta SI + \mu S + \lambda SL) + \phi R + \beta SI \\ &\quad - (\gamma I + \mu I + \delta I) + \tau L + \lambda SL \\ &\quad - (\mu L + \tau L + \sigma L) + \gamma I - \mu R - \phi R + \sigma L\end{aligned}$$

Simplifying the terms, we obtain:

$$\frac{dN}{dt} = \pi - \mu(S + I + L + R) - \delta I$$

$$\frac{dN}{dt} = \pi - \mu N - \delta I$$

$$\frac{dN}{dt} \leq \pi - \mu N$$

By applying Gronwall's lemma, we get:

$$N(t) \leq \frac{\pi}{\mu} - \left(\frac{\pi - \mu N_0}{\mu}\right) e^{-\mu t} \quad \forall \quad t \geq 0$$

where N_0 represents the initial population value. This implies:

$$0 \leq N(t) \leq \frac{\pi}{\mu} \quad \forall \quad t \geq 0, \quad \text{if} \quad N(0) \leq \frac{\pi}{\mu}$$

Hence, the appropriate subset θ_t is:

$$\theta_t = \{(S, L, I, R) \in \mathbb{R}^{+4} : S + L + I + R \leq \frac{\pi}{\mu}\}$$

So the equations in the model create a dynamical system which is bounded, and the system stay within a specific area or region [15, 16]. We can describe this area as follows:

$$\Delta = \theta_S + \theta_L + \theta_I + \theta_R$$

From this, we can conclude that the model's behavior in this area makes sense mathematically. Let's consider what happens when we start with all positive numbers in our system–that is, when all our starting values are greater than zero. In this case, as time goes on, our system will always give us positive answers. It won't suddenly jump to negative numbers or zero in the future.

3.2. Disease-free equilibrium point

Starting with the susceptible sub-population, we have:

$$\frac{dS}{dt} = \pi - \beta SI - \mu S - \lambda SL + \phi R = 0$$

Since $I = 0$, $L = 0$, and $R = 0$, this equation simplifies to:

$$S^* = \frac{\pi}{\mu}$$

Therefore, the disease-free equilibrium (DFE) is:

$$(S^*, I^*, L^*, R^*) = \left(\frac{\pi}{\mu}, 0, 0, 0\right) \tag{3}$$

3.3. Disease endemic equilibrium point

The endemic equilibrium point is obtained by solving the following system of equation;

$$\begin{cases} \pi - \beta SI - \mu S - \lambda SL + \phi R = 0 & (a) \\ \lambda SL - \mu L - \tau L - \sigma L = 0 & (b) \\ \beta SI - \gamma I - \mu I - \delta I + \tau L = 0 & (c) \\ \gamma I - \mu R - \phi R + \sigma L = 0 & (d) \end{cases}$$

From Equation (c):

$$\lambda S^* L^* - \mu L^* - \tau L^* - \sigma L^* = 0$$

we have:

$$L^*(\lambda S^* - \mu - \tau - \sigma) = 0$$

This implies:

$$L^* = 0 \quad \text{or} \quad S^* = \frac{\mu + \tau + \sigma}{\lambda}$$

From the Equation (b):

$$\beta S^* I^* - \gamma I^* - \mu I^* - \delta I^* + \tau L^* = 0$$

Substituting $S^* = \frac{\mu+\tau+\sigma}{\lambda}$:

$$I^*\left(\beta\frac{\mu + \tau + \sigma}{\lambda} - \gamma - \mu - \delta\right) + \tau L^* = 0$$

Let $a = \beta \frac{\mu+\tau+\sigma}{\lambda} - \gamma - \mu - \delta$. Thus:

$$aI^* + \tau L^* = 0$$

$$L^* = -\frac{aI^*}{\tau}$$

From the Equation (d):

$$\gamma I^* + \sigma L^* - (\mu + \phi)R^* = 0$$

Thus:

$$R^* = \frac{\gamma I^* + \sigma L^*}{\mu + \phi}$$

From the Equation (a):

$$\pi - \beta S^* I^* - \mu S^* - \lambda S^* L^* + \phi R^* = 0$$

Substituting $S^* = \frac{\mu+\tau+\sigma}{\lambda}$ and $L^* = -\frac{aI^*}{\tau}$:

$$\pi - \beta \left(\frac{\mu+\tau+\sigma}{\lambda}\right) I^* - \mu \left(\frac{\mu+\tau+\sigma}{\lambda}\right) - (\mu+\tau+\sigma)L^* + \phi \left(\frac{\gamma I^* + \sigma L^*}{\mu+\phi}\right) = 0$$

Let $b = \beta \left(\frac{\mu+\tau+\sigma}{\lambda}\right)$, $c = \mu \left(\frac{\mu+\tau+\sigma}{\lambda}\right)$, $d = \frac{a(\mu+\tau+\sigma)}{\tau}$:

$$\pi - bI^* - c + adI^* + \frac{\phi(\gamma I^* - \sigma a I^*/\tau)}{\mu+\phi} = 0$$

Combining the results to solve for I^*:

$$I^* \left(a + \phi \left(\frac{\gamma}{\mu+\phi}\right) - \frac{\sigma a}{\tau}\right) = \pi - c$$

Simplifying the terms involving I:

$$I^* \left[a + \frac{\phi\gamma}{\mu+\phi} - \frac{\sigma a}{\tau}\right] = \pi - c$$

Thus:

$$I^* = \frac{\pi - c}{a + \frac{\phi\gamma}{\mu+\phi} - \frac{\sigma a}{\tau}}$$

The Endemic Equilibrium Points are:

$$S^* = \frac{\mu+\tau+\sigma}{\lambda}$$
$$L^* = -\frac{a\left(\frac{\pi-c}{a+\frac{\phi\gamma}{\mu+\phi}-\frac{\sigma a}{\tau}}\right)}{\tau}$$
$$I^* = \frac{\pi-c}{a+\frac{\phi\gamma}{\mu+\phi}-\frac{\sigma a}{\tau}}$$
$$R^* = \frac{\gamma\left(\frac{\pi-c}{a+\frac{\phi\gamma}{\mu+\phi}-\frac{\sigma a}{\tau}}\right)+\sigma\left(-\frac{a\left(\frac{\pi-c}{a+\frac{\phi\gamma}{\mu+\phi}-\frac{\sigma a}{\tau}}\right)}{\tau}\right)}{\mu+\phi}$$

This disease endemic Equilibrium point exist if and only if, $\frac{a\left(\frac{\pi-c}{a+\frac{\phi\gamma}{\mu+\phi}-\frac{\sigma a}{\tau}}\right)}{\tau} > 0$, $\frac{\pi-c}{a+\frac{\phi\gamma}{\mu+\phi}-\frac{\sigma a}{\tau}} > 0$ where $a = \beta\frac{\mu+\tau+\sigma}{\lambda} - \gamma - \mu - \delta$ [17,18].

4. Basic reproduction number

Using the Jacobian Matrix approach in [19, 20] of the associated infectious compartments of the system of differential equations obtained from the model:

$$\frac{dI}{dt} = \beta SI - (\gamma+\mu+\delta)I + \tau L$$
$$\frac{dL}{dt} = \lambda SL - (\mu+\tau+\sigma)L$$

Applying the next generation matrix approach [21–23], then the basic reproduction number R_0 is given by :

$$K = FV^{-1}$$

and

$$R_0 = \rho(FV^{-1})$$

$$\rho(A) = \sup|\lambda| : \lambda \in \rho(A)$$

where this $\rho(A)$ represent every eigenvalues of matrix A.

$$f = \begin{pmatrix}\beta SI+\tau L\\ \lambda SL\end{pmatrix} and \quad v = \begin{pmatrix}(\gamma+\mu+\delta)I\\ (\mu+\tau+\sigma)L\end{pmatrix}$$

The Jacobian matrix J of the system given by:

$$J = \begin{pmatrix}\frac{\partial f}{\partial I} & \frac{\partial f}{\partial L}\\ \frac{\partial g}{\partial I} & \frac{\partial g}{\partial L}\end{pmatrix}$$

The next-generation matrix K is derived from the Jacobian. We decompose the Jacobian J into two matrices parts: F (new infection's terms) and V (transition out

terms).

$$F = \begin{pmatrix} \beta S & \tau \\ 0 & \lambda S \end{pmatrix}$$

$$V = \begin{pmatrix} \gamma+\mu+\delta & \tau \\ 0 & \mu+\tau+\sigma \end{pmatrix}$$

At the point of disease free equilibrium $S = S^*$. so the jacobian at disease free equilibrium would be; the next-generation matrix K is derived from the Jacobian at DFE. We decompose the Jacobian J into two matrices: F (new infection's terms) and V (transition out terms).

$$F(S^*,0,0,0) = \begin{pmatrix} \beta S^* & \tau \\ 0 & \lambda S^* \end{pmatrix}$$

$$V(S^*,0,0,0) = \begin{pmatrix} \gamma+\mu+\delta & 0 \\ 0 & \mu+\tau+\sigma \end{pmatrix}$$

Now we find the Inverse of V as:

$$V^{-1} = \frac{1}{(\gamma+\mu+\delta)(\mu+\tau+\sigma)} \begin{pmatrix} \mu+\tau+\sigma & 0 \\ 0 & \gamma+\mu+\delta \end{pmatrix}$$

next, we Calculate K

$$K = FV^{-1}$$

$$K = \begin{pmatrix} \beta S^* & 0 \\ 0 & \lambda S^* \end{pmatrix} \cdot \frac{1}{(\gamma+\mu+\delta)(\mu+\tau+\sigma)} \begin{pmatrix} \mu+\tau+\sigma & 0 \\ 0 & \gamma+\mu+\delta \end{pmatrix}$$

The eigenvalues of K give us the reproduction number. The eigenvalues are:

$$\frac{\beta S^*(\mu+\tau+\sigma)}{(\gamma+\mu+\delta)(\mu+\tau+\sigma)}$$

and

$$\frac{\lambda S^*(\gamma+\mu+\delta)}{(\gamma+\mu+\delta)(\mu+\tau+\sigma)}$$

Simplifying, we find:

$$R_0 = \sum \left(\frac{\beta S^*}{\gamma+\mu+\delta}, \frac{\lambda S^*}{\mu+\tau+\sigma} \right)$$

Thus, our basic reproduction number R_0 for the model, is the sum of the two eigenvalues:

$$R_0 = \left(\frac{\beta S^*}{\gamma+\mu+\delta} + \frac{\lambda S^*}{\mu+\tau+\sigma} \right) \tag{4}$$

or equivalently;

$$R_0 = \frac{\pi}{\mu} \left(\frac{\beta}{\gamma+\mu+\delta} + \frac{\lambda}{\mu+\tau+\sigma} \right)$$

5. Local stability of the DFE

To determine the stability of the system at equilibrium point, we use jacobian of the system of equation given by:

$$J = \begin{bmatrix} \frac{\partial f}{\partial S} & \frac{\partial f}{\partial I} & \frac{\partial f}{\partial L} & \frac{\partial f}{\partial R} \\ \frac{\partial g}{\partial S} & \frac{\partial g}{\partial I} & \frac{\partial g}{\partial L} & \frac{\partial g}{\partial R} \\ \frac{\partial h}{\partial S} & \frac{\partial h}{\partial I} & \frac{\partial h}{\partial L} & \frac{\partial h}{\partial R} \\ \frac{\partial k}{\partial S} & \frac{\partial k}{\partial I} & \frac{\partial k}{\partial L} & \frac{\partial k}{\partial R} \end{bmatrix} \tag{5}$$

Taking the jacobian of the system, we have:

$$J = \begin{bmatrix} -\beta I - \mu - \lambda L & -\beta S & -\lambda S & \phi \\ \beta I & \beta S - \gamma - \mu - \delta & \tau & 0 \\ \lambda L & 0 & -\mu - \tau - \sigma & 0 \\ 0 & \gamma & \sigma & -\mu - \phi \end{bmatrix} \tag{6}$$

Expressing the jacobian, at disease free equilibrium point [24,25],

$$J_{DFE} = J(\frac{\pi}{\mu},0,0,0) = \begin{bmatrix} -\mu & -\beta\frac{\pi}{\mu} & -\lambda\frac{\pi}{\mu} & \phi \\ 0 & \beta\frac{\pi}{\mu} - \gamma - \mu - \delta & 0 & 0 \\ 0 & 0 & \lambda\frac{\pi}{\mu} - \mu - \tau - \sigma & 0 \\ 0 & \gamma & \sigma & -\mu - \phi \end{bmatrix}$$

$$J(\frac{\pi}{\mu},0,0,0) = \begin{bmatrix} -\mu & -\beta\frac{\pi}{\mu} & -\lambda\frac{\pi}{\mu} & \phi \\ 0 & \beta\frac{\pi}{\mu} - (\gamma+\mu+\delta) & \tau & 0 \\ 0 & 0 & \lambda\frac{\pi}{\mu} - (\mu+\tau+\sigma) & 0 \\ 0 & \gamma & \sigma & -(\mu+\phi) \end{bmatrix} \tag{7}$$

Finding the eigenvalues of the jacobian at disease free equilibrium,

$$J(\frac{\pi}{\mu},0,0,0) = \begin{bmatrix} -\mu-\lambda_1 & -\beta\frac{\pi}{\mu} & -\lambda\frac{\pi}{\mu} & \phi \\ 0 & \beta\frac{\pi}{\mu} - (\gamma+\mu+\delta) - \lambda_2 & \tau & 0 \\ 0 & 0 & \lambda\frac{\pi}{\mu} - (\mu+\tau+\sigma) - \lambda_3 & 0 \\ 0 & \gamma & \sigma & -(\mu+\phi) - \lambda_4 \end{bmatrix}$$

The eigenvalues are;

$$\lambda_1 = -\mu$$
$$\lambda_2 = \beta\frac{\pi}{\mu} - (\gamma+\mu+\delta)$$
$$\lambda_3 = \lambda\frac{\pi}{\mu} - (\mu+\tau+\sigma)$$
$$\lambda_4 = -(\mu+\phi)$$

The DFE is locally asymptotically stable if $\beta\frac{\pi}{\mu} < (\gamma+\mu+\delta)$, $\lambda\frac{\pi}{\mu} < (\mu+\tau+\sigma)$ and $R_0 < 1$ [26–28].

6. Global stability of endemic equilibrium

To understand how the disease behaves when it's always present in the population, we'll use a special mathematical tool. This tool is called a Lyapunov function [29–33]. Let's create one:

$$L(S^*,I^*,L^*,R^*) = \begin{cases} (S-S^*-S^*\ln(\frac{S^*}{S})) + (I-I^*-I^*\ln(\frac{I^*}{I})) + (L-L^*-L^*\ln(\frac{L^*}{L})) \\ +(R-R^*-R^*\ln(\frac{R^*}{R})) \end{cases}$$

The rate of change of the function(derivative) L, calculated by following;

$$\frac{dL(S^*,I^*,L^*,R^*)}{dt} = \begin{cases} (\frac{S-S^*}{S})\frac{dS}{dt} + (\frac{I-I^*}{I})\frac{dI}{dt} + (\frac{L-L^*}{L})\frac{dL}{dt} + (\frac{R-R^*}{R})\frac{dR}{dt} \end{cases}$$

$$\frac{dL(S^*,I^*,L^*,R^*)}{dt} = \begin{cases} (\frac{S-S^*}{S})(\pi-\beta SI-\mu S-\lambda SL+\phi R) \\ +(\frac{I-I^*}{I})(\beta SI-\gamma I-\mu I-\delta I+\tau L) \\ +(\frac{L-L^*}{L})(\lambda SL-\mu L-\tau L-\sigma L) \\ +(\frac{R-R^*}{R})(\gamma I-\mu R-\phi R+\sigma L) \end{cases}$$

Expanding and simplifying the expressions gives;

$$\begin{cases} \pi-\beta SI-\mu S-\lambda SL+\phi R-\frac{\pi S^*}{S}+\beta S^*I+\lambda S^*L-\frac{\phi RS^*}{S}+\mu S^* \\ +\beta SI-\gamma I-\mu I-\delta I+\tau L-\beta SI^*+(\gamma+\mu+\delta)I^*-\frac{\tau LI^*}{I} \\ +\lambda SL-\mu L-\tau L-\sigma L-\lambda SL^*+(\tau+\sigma+\mu)L^* \\ +\gamma I-\mu R-\phi R+\sigma L-\frac{(\gamma I+\sigma L)R^*}{R}+(\phi+\mu)R^* \end{cases}$$

Let

$$\frac{dL}{dt} = P\text{-}Q$$

In this function, we have two main parts. Where P part are the positive terms, and Q part are the negative terms, such that:

$$\begin{aligned} P = {} & \pi + \phi R + (\beta I + \lambda L + \mu)S^* + \beta SI + \tau L \\ & + (\gamma + \mu + \delta)I^* + \lambda SL + (\tau + \sigma + \mu)L^* \\ & + \gamma I + \sigma L + (\phi + \mu)R^* \end{aligned}$$

$$\begin{aligned} Q = {} & (\beta I + \mu + \lambda L)S + \frac{\phi RS^*}{S} + (\gamma + \mu + \delta)I \\ & + \beta SI^* + \frac{\tau LI^*}{I} + (\mu + \tau + \sigma)L \\ & + \lambda SL^* + \mu R + \frac{(\gamma I + \sigma L)R^*}{R} \end{aligned}$$

$$\text{If} \quad P < Q, \quad \text{then} \quad \frac{dL}{dt} \leq 0$$

To ensure our Lyapunov function is valid, the necessary and sufficient condition for

$$\frac{dL}{dt} = 0 \quad \text{is when} \quad S = S^*,\ I = I^*,\ L = L^*,\ R = R^*$$

The maximal invariant set within the space defined by the variables S^*, I^*, L^*, and R^*, where the derivative of the lyapunuv function L with respect to time t is equal to zero, is a singleton set containing only the endemic equilibrium point E^* .This condition signifies that, the endemic equilibrium is globally and asymptotically stable [34–38].

7. Sensitivity analysis

To determine how much each part of our model affects the spread of the disease in relation to the basic reproduction number R_0, a sensitivity analysis is performed [39–42]. The sensitivity analysis is given by:

$$S_x^{R_0} = \frac{\partial R_0}{x} \times \frac{x}{R_0}$$

where x represent any parameter in the reproduction number.

$$R_0 = \left(\frac{\beta S^*}{\gamma + \mu + \delta}\right) + \left(\frac{\lambda S^*}{\mu + \tau + \sigma}\right)$$

Sensitivity index for β:

$$S_\beta^{R_0} = \frac{\partial R_0}{\beta} \times \frac{\beta}{R_0} = \left[\frac{S^*}{\gamma + \mu + \delta}\right] \times \left[\frac{\beta}{R_0}\right]$$

Sensitivity index for γ:

$$S_\gamma^{R_0} = \frac{\partial R_0}{\gamma} \times \frac{\gamma}{R_0} = -\frac{\beta S^*}{(\gamma + \mu + \delta)^2} = -\left[\frac{\beta S^*}{(\gamma + \mu + \delta)^2}\right] \times \left[\frac{\gamma}{R_0}\right]$$

Sensitivity index for μ:

$$S_\mu^{R_0} = \frac{\partial R_0}{\mu} \times \frac{\mu}{R_0} = -\frac{\beta S^*}{(\gamma + \mu + \delta)^2} - \frac{\lambda S^*}{(\mu + \tau + \sigma)^2} \times \frac{\mu}{R_0}$$

Sensitivity index for δ:

$$S_{\delta}^{R_0} = \frac{\partial R_0}{\delta} \times \frac{\delta}{R_0} - \frac{\beta S^*}{(\gamma+\mu+\delta)^2} = \left(\frac{\partial R_0}{\partial \delta}\right) \times \left(\frac{\delta}{R_0}\right) = \left[-\frac{\beta S^*}{(\gamma+\mu+\delta)^2}\right] \times \left[\frac{\delta}{R_0}\right]$$

Sensitivity index for λ:

$$S_{x}^{R_0} = \frac{\partial R_0}{\lambda} \times \frac{\lambda}{R_0} = \left(\frac{\partial R_0}{\partial \lambda}\right) \times \left(\frac{\lambda}{R_0}\right) = \left[\frac{S^*}{\mu+\tau+\sigma}\right] \times \left[\frac{\lambda}{R_0}\right]$$

Sensitivity index for τ:

$$S_{\tau}^{R_0} = \frac{\partial R_0}{\tau} \times \frac{\tau}{R_0} = \left(\frac{\partial R_0}{\partial \tau}\right) \times \left(\frac{\tau}{R_0}\right) = \left[-\frac{\lambda S^*}{(\mu+\tau+\sigma)^2}\right] \times \left[\frac{\tau}{R_0}\right]$$

Sensitivity index for σ:

$$S_{\sigma}^{R_0} = \frac{\partial R_0}{\sigma} \times \frac{\sigma}{R_0} = \left(\frac{\partial R_0}{\partial \sigma}\right) \times \left(\frac{\sigma}{R_0}\right) = \left[-\frac{\lambda S^*}{(\mu+\tau+\sigma)^2}\right] \times \left[\frac{\sigma}{R_0}\right]$$

All the Sensitivity indices of the model's parameters can be viewed in the table below.

The sensitivity analysis presented in **Table 3** reveals the impact of various model parameters on the basic reproduction number R_0 of the disease. Each parameter is associated with either a positive $(+)$ or negative $(-)$ sensitivity index, indicating its effect on R_0.

Table 3. Parameter values and their sensitivity indices

Parameter	Value	Reference
β	0.069	[1]
μ	-0.0047	[44]
λ	0.100	[7]
τ	-0.12	[7]
δ	-0.16	[43]
σ	-0.008	Assume [44]
γ	-0.08	[43]
π	0.00133	[43]

Specifically: The parameters β and λ have positive sensitivity indices. This means that an increase in these parameters leads to an increase in R_0, potentially worsening the spread of the disease. The parameters μ, μ, δ, σ, and γ all have negative sensitivity indices. This indicates that increasing these parameters results in a decrease in R_0, which could help in controlling the disease's spread.

These results provide valuable insights into which factors most significantly influence the disease's transmission dynamics. Parameters with positive indices might be targets for intervention strategies aimed at reducing disease spread, while those with negative indices could be leveraged to enhance control efforts.

This analysis not only helps in understanding the relative importance of different factors in disease transmission but also guides the development of effective strategies

for disease control and prevention.

8. Numerical simulation

A numerical simulation was conducted to explore the impact of various parameters on the tuberculosis model. This approach approximated solutions for coupled differential equations, allowing for analysis of how changes in parameter values affected the system dynamics [45–49]. The simulation focused on a system of differential equations from the model in **Figure 4.1**, representing four human population compartments: susceptible, Infected, Latent and Recovered.

The primary goal was to observe the evolution of these population compartments over time. The simulation aimed to provide insights into the progression of tuberculosis and the impact of interventions or parameter changes on population dynamics.The simulation used specific parameter values, detailed in the accompanying **Table 4**. These values were crucial in determining the dynamics of the tuberculosis epidemic over a one-month period.

To illustrate the dynamics, a graph was generated using the simulated data. This graph depicted the changes in each population compartment over time during the specified tuberculosis epidemic period. The simulation aimed to provide insights into the progression of the disease and the impact of interventions or changes in parameter values on population dynamics.

To visually illustrate these dynamics, graphs were generated using the simulated data. This graph depicted how each population compartment changed over time during the specified tuberculosis epidemic period. These visualizations are crucial for understanding the role of each compartment and for informing decision-making processes related to disease control and management strategies.

Table 4. Parameter values used for the simulation

Parameter	Value	Reference
β	0.069	[1]
μ	0.0047	[44]
λ	0.100	[7]
τ	0.12	[7]
δ	0.16	[43]
σ	0.008	Assume [44]
γ	0.08	[43]
ϕ	0.018	[43]
π	0.00133	[43]

Table 4 is the parameter values are used in the numerical simulation. The results of the numerical simulation are presented in **Figures 2–5**.

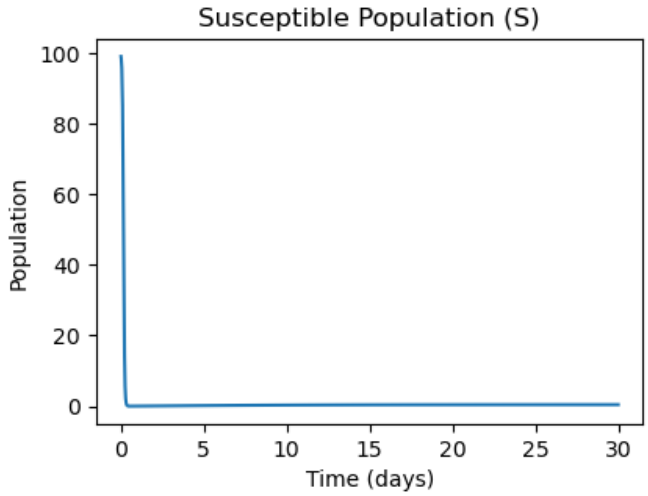

Figure 2. The susceptible population.

Based on the graph in **Figure 2**, we can see that the susceptible population initially starts at a higher level, as we assumed a population of 100 ($S_0 = 100$), but gradually decreases as individuals become infected or transition to the latent stage. The rate of decrease in the susceptible population is influenced by the relatively low transmission rate ($\beta = 0.069$), which indicates that the disease is not spreading rapidly through contact in the population. Additionally, the rate of progression to the latent stage ($\lambda = 0.100$) indicates that not all susceptible individuals become infected with the disease. Therefore, as the epidemic progresses, the susceptible population continues to decline due to disease transmission and the transition to the latent stage. However, the susceptible population might eventually start to increase again due to the influx of new recruits (incidence rate π) and the recovery of individuals who lose immunity (ϕ).

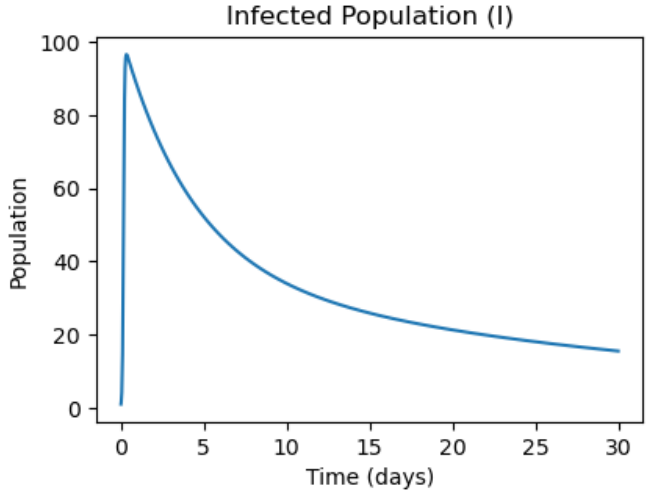

Figure 3. Infected population

Figure 3 shows that, an infected population starts from a small portion of the population ($I_0 = 1$), and initially increases as the disease spreads through the susceptible population. This increase in the infected population depends is influenced by the transmission rate β, and the rate of progression from the latent stage to the infected

stage τ. After reaching a peak at some certain stage, the infected population starts to decline due to individuals recovering from the disease at a very high recovery rate γ, died naturally μ or died due to the disease δ. This result in the declining of the infected individuals leading to the disease free stage in the population.

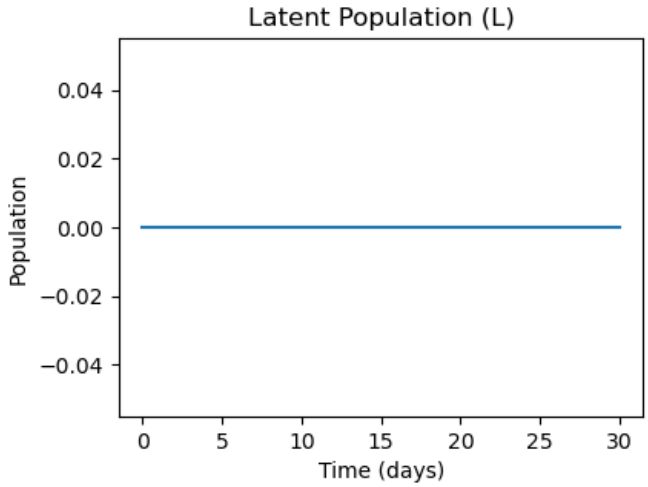

Figure 4. Latent Population

The latent population initially starts at zero $(L_0 = 0)$ but gradually increases as susceptible individuals transition to the latent stage at rate λ. The rate of increase in the latent population is determined by the rate of progression to the latent stage λ and the size of the susceptible population as shown in **Figure 4**. After reaching a peak, the latent population starts to decline and move in a constant level, as individuals progress to the infected stage, died, recovered directly from the latent stage at the rate σ. This constant movement in the latent population is due to the balance in between the rates of progression to the infected stage τ and the recovery rate from the latent stage σ natural dead μ and the size of susceptible population.

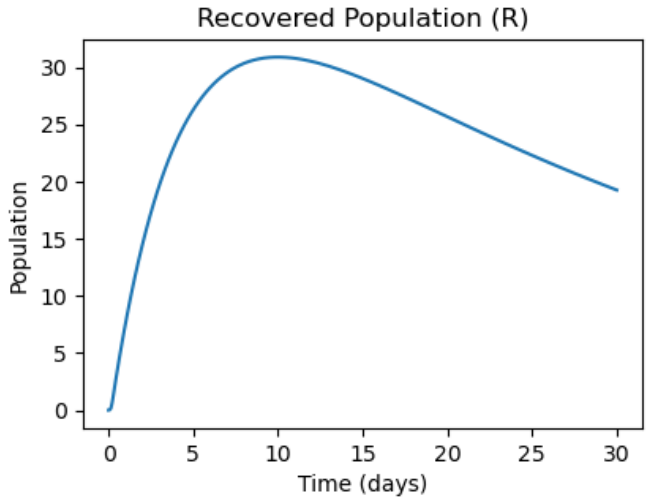

Figure 5. Recovered Population

The recovered population starts initially at zero $(R = 0)$ and subsequently increased as infected individuals recovered from the disease at a very higher rate

γ as shown in **Figure 5**. This increase in the recovered individuals is influenced by the size of the infected population which loses its peak due the recovery rate γ. After reaching a peak, the recovered population will eventually starts to decline due to individuals losing immunity and becoming susceptible again with the rate ϕ, and also the natural death rate μ.

9. Conclusion

To explore potential avenues for tuberculosis eradication, it is imperative to delve into its transmission dynamics and prevalence. Many infectious diseases, including tuberculosis, have been effectively studied using differential equations. This thesis has focused on analyzing and modeling the transmission dynamics of tuberculosis, considering both latent and active populations. We have developed a mathematical model aimed at elucidating these dynamics, investigating key parameters such as the reproductive number, equilibrium points, and their stability. Additionally, sensitivity analysis has been performed to assess the contribution of each parameter on the reproductive number. Numerical simulations using established parameters have further illustrated the population dynamics of the disease, supported by graphical representations generated using appropriate software.

We assumed that the population has a constant size *N*, where births and deaths occur at equal rates, and that newborns are also susceptible to the disease. Additionally, there is no age restriction, mobility, or other social factors. We also assumed that once infected with tuberculosis bacteria, an individual might become latent or directly infectious.

Based on the assumptions above, the dynamics of the tuberculosis model satisfy the SILR epidemiological model discussed in Chapter Four. Hence, we propose it to study the dynamic transmission of tuberculosis by classifying the population as susceptible (S), infectious (I), latent (L), and recovered (R).

All parameters used in the model are described in Chapter Four. The model has shown success in predicting the causes of transmission dynamic within a population. From the model analysis, we also observed that the dynamics of the susceptible population are influenced by the incidence rate (π), the transmission contact rate (β), which also facilitates the infection rate (βSI), the natural death rate (μS), the rate at which some individuals lose susceptibility and become latent (λSL), and the gain due to the lack of immunity from the recovered population (ϕR). This has been shown in the graph of the susceptible population. The susceptible population is initially high, but it decreases as individuals become infected, die, or move to the latent compartment.

The graph of infected population initially rises as susceptible individuals become infected, but it eventually decreases as some infected individuals die due to tuberculosis, some died naturally, while others recovered.

In the latent, the graph shows the change in the latent population over time. But the latent population initially increases as susceptible individuals become latently infected, but it eventually decreases as latent individuals recovered, died or become actively infected. this resulted in the constant movement of the individuals in this compartment.

The recovered population initially increases as infected individuals recover, but it

eventually decreases as recovered individuals become susceptible again due to lack of permanent immunity in the dynamic of tuberculosis or die naturally.

The model also provides an approximate reproduction number of 0.3, which epidemiologically demonstrates the impact of applying the SILR model in curtailing tuberculosis. The model indicates that even though the approximate calculated reproduction number $\mathscr{R}_0$ is less than unity, which suggests that tuberculosis will naturally decline in the population, there is a need to maintain the decrease in the transmission/infection rate β and improve the recovery rate γ so that the disease will eventually die out completely. Future work could focus on refining the model by including additional compartments, nonlinear dynamics, or more complex interaction terms. This can help better capture the complexity of the system or disease in real-world settings. The model could be tested with actual data from specific regions or populations to validate its predictions. This could help in assessing its predictive accuracy and adapting it to local conditions.

Author contributions:

Acknowledgments: Authors profoundly acknowledged the contribution of researchers in mathematical modelling for their immense suggestions.

Data availability: The data used in this study are taken from published work. These are cited as in text and referenced accordingly.

Conflict of interest: The authors declare no conflict of interest.

References

1. Bagcchi S. WHO's global tuberculosis report 2022. The Lancet Microbe. 2023; 4(1): e20.
2. Ojo MM, Peter OJ, Goufo EFD, et al. Mathematical model for control of tuberculosis epidemiology. Journal of Applied Mathematics and Computing. 2023; 69(1): 69–87.
3. Andam EA. Analysis of transmission dynamics of tuberculosis (TB) using differential equations: A case study of Amansie West District, Ghan [PhD thesis]. Kwame Nkrumah University of Science and Technology; 2013.
4. Frith J. History of tuberculosis. Part 1-phthisis, consumption and the white plague. Journal of Military and Veterans Health. 2014; 22(2): 29–35.
5. Otoo D, Osman S, Poku SA, Donkoh EK. Dynamics of tuberculosis (TB) with drug resistance to first-line treatment and leaky vaccination: A deterministic modelling perspective. Computational and Mathematical Methods in Medicine. 2021.
6. Bhunu CO, Garira W. A two strain tuberculosis transmission model with therapy and quarantine. Mathematical Modelling and Analysis. 2009; 14(3): 291–3129.
7. Kabunga SK, Goufo EFD, Tuong VH. Analysis and simulation of a mathematical model of tuberculosis transmission in democratic republic of the congo. Advances in Difference Equations. 2020; 2020(1): 642.
8. Otoo D, Osman S, Poku SA, Donkoh EK. Dynamics of tuberculosis (TB) with drug resistance to first-line treatment and leaky vaccination: A deterministic modelling perspective. Computational and Mathematical Methods in Medicine. 2021.
9. Osman S, Makinde OD. A mathematical model for coinfection of listeriosis and anthrax diseases. International Journal of Mathematics and Mathematical Sciences. 2018; 2018: 1725671. doi: 10.1155/2018/1725671
10. Otoo D, Abeasi IO, Osman S, Donkoh EK. Mathematical modeling and analysis of the dynamics of hepatitis B with optimal control. Communications in Mathematical Biology and Neuroscience. 2021; 2021: 43.
11. Osman S, Tilahun GT, Alemu SD, Onsongo WM. Analysis of the dynamics of rabies in North Shewa, Ethiopia. Italian Journal of Pure and Applied Mathematics. 2022; 48: 877–902.
12. Otoo D, Abeasi IO, Osman S, Donkoh EK. Stability analysis and modeling the dynamics of hepatitis B with vaccination

compartment. Italian Journal of Pure and Applied Mathematics. 2022; 48: 903–927.
13. Okosun KO, Mukamuri M, Makinde DO. Global stability analysis and control of leptospirosis. Open Mathematics. 2016; 14(1): 567–585.
14. Kayange HL, Massawe ES, Makinde DO, Immanuel LS. Modelling and Optimal Control of Ebola Virus Disease in the Presence of Treatment and Quarantine of Infectives. International Journal of Systems Science and Applied Mathematics. 2020; 5: 43.
15. Osman S, Togbenon HA, Otoo D. Modelling the dynamics of campylobacteriosis using nonstandard finite difference approach with optimal control. Computational and Mathematical Methods in Medicine. 2020; 2020: 8843299. doi: 10.1155/2020/8843299
16. Onsongo WM, Mwini ED, Nyanaro BN, Osman S. The dynamics of psittacosis in human and poultry populations: A mathematical modelling perspective. Journal of Mathematical and Computational Science. 2021; 11(6): 8472–8505.
17. Osman S, Makinde OD, Theuri DM. Mathematical modelling of listeriosis epidemics in animal and human population with optimal control. Tamkang Journal of Mathematics. 2020; 51(4): 261–287.
18. Otoo D, Tilahun GT, Osman S, Wole GA. Modeling the dynamics of tuberculosis with drug resistance in North Shoa Zone, Oromiya Regional State, Ethiopia. Communications in Mathematical Biology and Neuroscience. 2021; 2021: 12.
19. Eegunjobi AS, Makinde OD. Mathematical Analysis of Two Strains Covid-19 Disease Using SEIR Model. Journal of Mathematical & Fundamental Sciences. 2022; 54(2): 211–232.
20. Yano TK, Makinde OD, Malonza DM. Modelling childhood disease outbreak in a community with inflow of susceptible and vaccinated new-born. Global Journal of Pure and Applied Mathematics. 2016; 12(5): 3895–3916.
21. Osman S, Otoo D, Sebil C, Makinde OD. Bifurcation, sensitivity and optimal control analysis of modelling Anthrax-Listeriosis co-dynamics. Communications in Mathematical Biology and Neuroscience. 2020; 2020: 98.
22. Osman S. Otoo D, Sebil C, Makinde OD. Bifurcation, sensitivity and optimal control analysis of modelling anthrax-listeriosis co-dynamics. Communications in Mathematical Biology and Neuroscience. 2020; 2020: 98.
23. Osman S, Makinde OD, Theuri DM. Stability analysis and modelling of listeriosis dynamics in human and animal populations. Global Journal of Pure and Applied Mathematics. 2018; 14(1): 115–137.
24. Hugo A, Makinde OD, Kumar S. An eco-epidemiological model for Newcastle disease in central zone Tanzania. International Journal of Computing Science and Mathematics. 2019; 10(3): 215–235.
25. Massawe LN, Makinde OD. Parameter Estimation and Sensitivity Analysis of Bus Rapid Transit Frequency in Tanzania. International Journal of Transportation Engineering and Technology. 2023; 9(4): 79–85.
26. Otoo D, Tilahun GT, Osman S, Wole GA. Modeling the dynamics of tuberculosis with drug resistance in North Shoa Zone, Oromiya Regional State, Ethiopia. Communications in Mathematical Biology and Neuroscience. 2021; 2021: 12.
27. Osman S, Otoo D, Makinde OD, et al. Modeling anthrax with optimal control and cost effectiveness analysis. Applied Mathematics. 2020; 11(03): 255.
28. Osman S, Musyoki EM, Ndung'u RM. A mathematical model for the transmission of measles with passive immunity. International Journal of Research in Mathematical and Statistical Sciences. 2019; 6: 1–8.
29. Berhe HW, Makinde OD. Computational modelling and optimal control of measles epidemic in human population. Biosystems. 2020; 190: 104102.
30. Berhe HW, Makinde OD, Theuri DM. Modelling the dynamics of direct and pathogens-induced dysentery diarrhoea epidemic with controls. Journal of biological dynamics. 2019; 13(1): 192–217.
31. Muia DW, Osman S, Wainaina M. Modelling and analysis of trypanosomiasis transmission mechanism. Global Journal of Pure and Applied Mathematics. 2018; 14(10): 1311–1331.
32. Osman S, Otoo D, Sebi C. Analysis of listeriosis transmission dynamics with optimal control. Applied Mathematics. 2020; 11(7): 712–737.
33. Osman S, Makinde OD, Theuri DM. Stability analysis and modelling of listeriosis dynamics in human and animal populations. Global Journal of Pure and Applied Mathematics. 2018; 14(1): 115–137.
34. Keno TD, Dano LB, Makinde OD. Modeling and optimal control analysis for malaria transmission with role of climate variability. Computational and Mathematical Methods. 2022; 2022(1): 9667396.
35. Osman S, Makinde OD, Theuri DM. Mathematical modelling of transmission dynamics of anthrax in human and animal population. Mathematical Theory and Modelling. 2018.
36. Eustace KA, Osman S, Wainaina M. Mathematical modelling and analysis of the dynamics of cholera. Global Journal of Pure and Applied Mathematics. 2018; 14(9): 1259–1275.

37. Kanyaa JK, Osman S, Wainaina M. Mathematical modelling of substance abuse by commercial drivers. Global journal of pure and applied mathematics. 2018; 14(9): 1149–1165.
38. Karunditu JW, Kimathi G, Osman S. Mathematical modeling of typhoid fever disease incorporating unprotected humans in the spread dynamics. Journal of Advances in Mathematics and Computer Science. 2019; 32(3): 1–11.
39. Tessema H, Haruna I, Osman S, Kassa E. A mathematical model analysis of marriage divorce. Communications in Mathematical Biology and Neuroscience. 2022.
40. Eyaran WE, Osman S, Wainaina M. Modelling and analysis of seir with delay differential equation. Global Journal of Pure and Applied Mathematics. 2019; 15(4): 365–382.
41. Onsongo WM, Mwini ED, Nyanaro BN, Osman S. The dynamics of psittacosis in human and poultry populations: A mathematical modelling perspective. Journal of Mathematical and Computational Science. 2021; 11(6): 8472–8505.
42. Karanja TW, Osman S, Wainaina M. Analysis and modelling of ringworm infections in an environment. Global Journal of Pure and Applied Mathematics. 2019; 15(5): 649–665.
43. World Health Organization. Global tuberculosis report 2022. World Health Organization; 2022.
44. Central Intelligence Agency. The world factbook. Available online: https://www.cia.gov/the-world-factbook/field/death-rate/ (accessed on 10 October 2024).
45. Okosun KO, Mukamuri M, Makinde OD. Co-dynamics of trypanosomiasis and cryptosporidiosis. Applied Mathematics & Information Science. 2016; 10(6): 2137–2161.
46. Otoo D, Edusei H, Gyan A, et al. Optimal prevention of HIV-AIDS with emphasis on unprotected and unnatural canal activities: A deterministic modelling perspective. Communications in Mathematical Biology and Neuroscience. 2023.
47. Onsongo WM, Mwini ED, Nyanaro BN, Osman S. Stability analysis and modelling the dynamics of psittacosis in human and poultry populations. Communications in Mathematical Biology and Neuroscience. 2022.
48. Diallo B, Okelo JA, Osman S, et al. A study of fractional bovine tuberculosis model with vaccination on human population. Communications in Mathematical Biology and Neuroscience. 2023.
49. Konlan M, Abassawah Danquah B, Okyere E, et al. Global stability analysis and modelling onchocerciasis transmission dynamics with control measures. Infection Ecology & Epidemiology. 2024; 14(1): 2347941.